The Journal of Immunology

Chemerin Peptides Promote Phagocytosis in a ChemR23- and Syk-Dependent Manner

Jenna L. Cash, Annabel R. Christian and David R. Greaves

J. Immunol. 2010;184;5315-5324; originally published online Apr 2, 2010;
doi:10.4049/jimmunol.0903378
http://www.jimmunol.org/cgi/content/full/184/9/5315

The Journal of Immunology is published twice each month by The American Association of Immunologists, Inc., 9650 Rockville Pike, Bethesda, MD 20814-3994.

Print ISSN: 0022-1767 Online ISSN: 1550-6606.

Chemerin Peptides Promote Phagocytosis in a ChemR23- and Syk-Dependent Manner

Jenna L. Cash, Annabel R. Christian, and David R. Greaves

Chemerin peptides represent a recently identified component of the endogenous anti-inflammatory network that act via the G protein-coupled receptor ChemR23. The role of the chemerin peptide/ChemR23 pathway in phagocytosis, the clearance of apoptotic cells (efferocytosis), and the resolution of inflammation is unknown. In this article, we report that low picomolar concentrations of the chemerin peptide chemerin15 (C15) enhance macrophage (MΦ) phagocytosis of microbial particles and apoptotic cells by up to 360% in vitro. These prophagocytic effects of C15 are significantly impaired in ChemR23$^{-/-}$ MΦs and are associated with increased actin polymerization and localization of F-actin to the phagocytic cup. Importantly, pharmacological inhibition of Syk activity completely abrogates the prophagocytic activities of C15 and associated changes in actin polymerization and phagocytic cup formation, suggesting that C15 promotes phagocytosis by facilitating phagocytic cup development in a Syk-dependent manner. During peritoneal inflammation, C15 administration (8 pg/mouse) enhances microbial particle clearance and apoptotic neutrophil ingestion by MΦs in wild-type but not ChemR23$^{-/-}$ mice, such that levels of apoptotic and necrotic cells at the inflammatory site are profoundly reduced. In contrast, neutralization of endogenous chemerin species during peritoneal inflammation significantly impairs MΦ ingestion of apoptotic neutrophils and zymosan. Our data identify a key role of the chemerin peptide/ChemR23 axis in the efficient clearance of foreign material, efferocytosis, and, hence, the resolution of inflammation. Manipulation of the chemerin peptide/ChemR23 axis may represent a novel therapeutic approach for the treatment of inflammatory pathologies, especially if failure to efficiently clear phagocytic targets has been implicated in their pathogenesis.
***The Journal of Immunology*, 2010, 184: 5315–5324.**

Macrophages (MΦs) are innate immune cells that can recognize, phagocytose, and kill microbial pathogens; as such, they represent an important component of the body's defense against infection (1–3). Efficient clearance of pathogenic material by MΦs is important in limiting the magnitude and duration of the ensuing inflammatory response, although recognition and engulfment of microbial particles by MΦs typically results in their activation and the secretion of inflammatory cytokines (4, 5). In contrast, MΦ ingestion of apoptotic cells is nonphlogistic (noninflammatory) because it does not provoke inflammatory mediator expression and is associated with active suppression of proinflammatory mediator release and upregulation of anti-inflammatory mediator expression, including TGF-β (6–9). Thus, apoptotic cell phagocytosis (efferocytosis) plays an important role in the resolution of inflammation and the maintenance of peripheral immune tolerance (1, 2, 7, 9, 10). Inefficient clearance of apoptotic cells, resulting in the accumulation of secondary necrotic cells, can result in the exacerbation of inflammation, because necrotic cell ingestion elicits MΦ activation, and necrotic cell lysis releases cytotoxic, proinflammatory, and immunogenic material (11–17). Thus, failure to efficiently clear apoptotic cells favors inflammatory and autoimmune reactions rather than inflammatory resolution, and it promotes a persistent state of inflammation seen in systemic lupus erythematosus (SLE), as well as in atherosclerosis and diabetes mellitus (18–22). Studies in experimental animal models combined with clinical evidence from human inflammatory diseases, including SLE, highlight the importance of efficient phagocytosis of apoptotic material during inflammation and also suggest its potential as a therapeutic target for the treatment of certain inflammatory diseases (12, 19, 20, 22–24).

We previously reported that picogram quantities of C-terminal peptides derived from the chemoattractant chemerin, in particular chemerin15 (C15; AGEDPHGYFLPGQFA), inhibit MΦ activation and suppress peritonitis induced by the yeast cell wall component zymosan (25). We hypothesized that chemerin peptides may achieve this effect, in part, by enhancing MΦ phagocytosis of the inciting stimulus, zymosan, and/or modulating the nonphlogistic ingestion of apoptotic cells at the site of inflammation.

In this study, we show for the first time that chemerin peptides potently and profoundly enhance MΦ clearance of microbial particles and apoptotic cells in a nonphlogistic and ChemR23-dependent manner, a process that requires Syk-dependent changes in F-actin polymerization and phagosome formation.

Materials and Methods

Animals

All animal studies were conducted with ethical approval from the Dunn School of Pathology Local Ethical Review Committee and in accordance with the U.K. Home Office regulations (Guidance on the Operation of Animals, Scientific Procedures Act, 1986). ChemR23$^{-/-}$ mice on an Sv129Ev background were a kind gift of Takeda (Cambridge, U.K.).

Sir William Dunn School of Pathology, University of Oxford, Oxford, United Kingdom

Received for publication October 14, 2009. Accepted for publication March 3, 2010.

This work was supported by the British Heart Foundation Grants RG/05/011 (to D.R.G.) and FS/05/121 (to J.L.C.).

Address correspondence and reprint requests to Dr. David R. Greaves, Sir William Dunn School of Pathology, Oxford University, South Parks Road, Oxford OX1 3RE, United Kingdom. E-mail address: david.greaves@path.ox.ac.uk

The online version of this paper contains supplemental material.

Abbreviations used in this paper: ChAb, neutralizing anti-chemerin Ab; C15, chemerin15; C15-S, scrambled C-15 peptide; GeoMFI, geometric mean fluorescence intensity; MΦ, macrophage; OpZ, serum-opsonized zymosan; PEC, peritoneal exudate cell; PI, propidium iodide; PIC, piceatannol; RRI, relative recognition index; SLE, systemic lupus erythematosus.

MΦ culture and zymosan phagocytosis assays

MΦs were obtained and cultured, as previously described (25). Briefly, Bio-Gel P100 polyacrylamide beads (1 ml 2% w/v in PBS; Bio-Rad, Hemel Hempstead, U.K.) were injected into the peritoneal cavities of 8–12-wk-old C57BL/6 mice. Mice were killed 4 d later, and peritoneal exudate cells (PECs) were collected in PBS 2 mM EDTA (Lonza, Slough, U.K.). Harvested cells were centrifuged and resuspended in OptiMEM supplemented with 2 mM L-glutamine, 50 U/ml penicillin, and 50 μg/ml streptomycin (all from Invitrogen, Paisley, U.K.). Cells were plated in 24-well suspension plates (0.4×10^6/well; Greiner Bio-One, Stonehouse, U.K.) and allowed to adhere for 1 h at 37°C in a humidified atmosphere containing 5% CO_2 to purify MΦ populations by adherence. Nonadherent cells and Bio-Gel beads were removed by washing with PBS after 1 h. MΦs were preincubated with 10^{-13}–10^{-9} M C15 (Biosynthesis, Lewisville, TX), C15-S (scrambled C15 peptide; GLFHDQAGPPAGYEF; Biosynthesis), or chemerin (R&D Systems, Minneapolis, MN) for 45 min at 37°C and then transferred to ice for 10 min prior to the addition of zymosan-FITC (Invitrogen) or serum-opsonized zymosan (OpZ)-FITC in a 10:1 ratio (zymosan: MΦ). Cells were challenged with zymosan/OpZ-FITC for 5, 15, 30, 45, or 60 min at 37°C, and the assay was terminated by transferring cells to ice and vigorously washing off noningested material with ice-cold PBS four times. Cells were lifted from tissue culture plastic using lidocaine-EDTA (Sigma-Aldrich, St. Louis, MO) and scraping and were fixed using 4% v/v formalin. In control experiments, fluorescence from extracellularly bound FITC particles was neutralized by quenching with trypan blue. The addition of trypan blue and the reconstruction of individual Z-series confocal images confirmed that extracellularly bound particles were not present following stringent washing. Opsonized FITC-zymosan was generated by incubating zymosan-FITC (20 mg/ml) and 100% mouse serum in a 1:1 v/v ratio for 1 h at 37°C with gentle shaking. The OpZ was then washed three times in PBS to remove excess serum. Where appropriate, the Syk inhibitor, piceatannol (PIC; 10 μM; Tocris Cookson, Bristol, U.K.), was administered 20 min before C15 pretreatment. Results obtained with PIC were confirmed using a second Syk inhibitor, BAY 61-3606 (1 μM; Sigma-Aldrich; data not shown). Lack of cytotoxicity of 10 μM PIC and 1 μM BAY 61-3606 was determined using CellTiter-Glo assay (Promega, Madison, WI). In separate experiments, the effect of C15 treatment on MΦ binding of zymosan was determined by pretreating with C15 at 37°C and then performing the above phagocytosis assay at 4°C. All in vitro experiments were performed in OptiMEM supplemented as described above, and all peptides were reconstituted in filter-sterilized PBS 0.1% BSA. Data from all in vitro phagocytosis assays are expressed as a relative recognition index (RRI), as described below.

For collection of MΦ supernatants, the above zymosan-phagocytosis assays were carried out in six-well plates (1×10^6 cells/well; Costar, Loughborough, U.K.) with C15 pretreatment (45 m), followed by stimulation with unlabeled zymosan (Sigma-Aldrich) in a 10:1 ratio for 15 min. Noningested zymosan was removed by washing on ice with cold PBS, after which 2 ml supplemented OptiMEM was added to each well, and cells were incubated for 15 h at 37°C. MΦ supernatants were then collected and stored at −80°C until use in Luminex assays (Bio-Rad).

Measurement of apoptosis

Jurkat cells were cultured in RPMI 1640 (PAA Laboratories, Yeovil, U.K.) with 10% FCS (PAA Laboratories), 1 mM sodium pyruvate (Invitrogen), 10 mM HEPES (Invitrogen), 0.05 mM β-mercaptoethanol (Sigma-Aldrich), 50 U/ml penicillin, and 50 μg/ml streptomycin. Apoptotic Jurkat cells were generated by UV irradiation (20–30 mJ/cm^2), followed by a 4-h incubation at 37°C in serum-free media. The percentage of apoptosis was assessed by staining 5×10^5 cells for 15 min with 0.5 μg propidium iodide (PI; Sigma-Aldrich) and 5 μl Annexin V-FITC (BD Biosciences) and performing FACS analysis in accordance with published protocols. Typically, 70% of Jurkat cells had undergone apoptosis using this protocol; therefore, they were Annexin-V$^+$PI$^-$.

Apoptotic cell phagocytosis assays

Following the induction of apoptosis, Jurkat cells were stained with CFSE (1 μM; Sigma-Aldrich) for 5 min and delivered to the MΦs in a 1:1 ratio after 45 min of pretreatment with 10^{-14}–10^{-11} M C15, C15-S, or chemerin. MΦs were exposed to apoptotic Jurkat cells for 1 h, and the assay was terminated as described above. In some cases, the serine and cysteine protease inhibitor leupeptin (15 μg/ml; Sigma-Aldrich) was added 20 min before chemerin pretreatment. For collection of MΦ supernatants, apoptotic cell-phagocytosis assays were carried out, as described above but in six-well plates (1×10^6 cells/well; Costar). MΦ supernatants were collected 15 or 24 h (TGF-β only) after removal of the phagocytic targets.

Calculation of the RRI

RRI was calculated using the equation RRI = % × (unknown geometric mean fluorescence intensity [GeoMFI])/(vehicle GeoMFI), where % is the percentage of zymosan-FITC$^+$ MΦs, OpZ-FITC$^+$ MΦs, or CFSE-labeled apoptotic cell$^+$ MΦs, and "unknown" GeoMFI is the GeoMFI of C15-, C15-S–, or chemerin-treated samples.

Detection of secreted proteins by ELISA and Luminex

TNF-α, IL-6 and -12 p40, and JE (MCP-1) concentrations in cell supernatants were assessed by Luminex multiplex bead assay (Bio-Rad), according to the manufacturer's instructions. Detection limits were 5–20 pg/ml, depending on the cytokine in question. TGF-β concentrations were determined by ELISA (R&D Systems; detection limit was 5 pg/ml).

F-actin staining and phagocytic cup formation

MΦs (1×10^6/well) were plated in six-well tissue culture plates (Costar) containing a 22-mm thickness 1 coverslip (VWR, Leighton, U.K.). Following MΦ adherence and removal of nonadherent cells, MΦs were treated with C15 for 45 min at 37°C; challenged with zymosan-FITC, as described above, for 5 min; and then transferred to ice where media were removed; cells were washed; and actin staining solution (4% v/v formalin in PBS, 5 U/ml Alexa Fluor 546-phalloidin [Invitrogen] and 5 mg/ml lysopalmitoylphosphatidylcholine [Sigma-Aldrich]) was added for 20 min. After 20 min on ice, the staining solution was removed, and cells were washed three times with cold PBS. Coverslips were mounted, and polymerized actin, phagocytic cups, and phagosomes were visualized by confocal microscopy. Early and late phagocytic cups and early phagosomes were judged from phalloidin-Alexa Fluor 546–stained images. Early phagocytic cups were defined as the presence of an actin cup-like structure around ~10–25% of the circumference of the zymosan particle. Late phagocytic cups were defined as the presence of an actin cup around ~50% of the zymosan particle. Phagosomes were defined by 100% enclosure of the zymosan particle by F-actin where early phagosomes were located at the cells periphery, and late phagosomes were found near the center of the cell.

In vivo phagocytosis

C57BL/6J mice were administered 500 μl C15 (0.32 ng/kg), C15-S (0.32 ng/kg), neutralizing anti-murine Chemerin Ab (ChAb, R&D Systems; 100 ng/mouse), control IgG (R&D Systems; 100 ng/mouse), or vehicle (PBS; Lonza) i.p. 1 h before injection of 500 μl 10 μg unlabeled zymosan (for Ly6G$^+$ cell phagocytosis; Sigma Aldrich) or zymosan-FITC (for zymosan phagocytosis; Invitrogen). For Ly6G$^+$ cell phagocytosis, PECs were collected by lavage with 5 ml PBS, 2 mM EDTA after 2, 4, 8, 16, or 24 h. For zymosan phagocytosis, PECs were collected after 0.5, 1, 2, or 4 h. PECs (1×10^6) were fixed (4% v/v formalin), permeabilized, and blocked (3% BSA [Sigma-Aldrich], 0.1% Triton X-100 [Sigma-Aldrich], 2.5 μg/ml 2.4G2 FcγII/III [AbD Serotec, Kidlington, U.K.]) prior to staining with F4/80-Alexa Fluor 647 (4 μg/ml; BD Biosciences, Oxford, U.K.) and Ly6G-PE (2 μg/ml, only for Ly6G$^+$ cell phagocytosis; BD Biosciences). Zymosan$^+$, F4/80$^+$, and Ly6G$^+$F4/80$^+$ cells, as a percentage of the total PECs and total F4/80$^+$ cells, were obtained using FlowJo (Tree Star, Ashland, OR).

ChAb effect on leukocyte recruitment

C57BL/6J mice were administered 500 μl ChAb (100 ng/mouse) or isotype control IgG (100 ng/mouse; both from R&D Systems) i.p. 1 h before i.p. injection of 500 μl 10 μg zymosan (Sigma-Aldrich). After 2, 4, 8, 16, 24, or 48 h and humane sacrifice, PECs were collected by peritoneal lavage with 5 ml sterile PBS-2 mM EDTA. Total cell counts were determined, and the percentage of neutrophils and monocytes in the peritoneal lavage fluid were obtained by FACS analysis, as previously described (25). Briefly, cells (1×10^5) were blocked with anti-mouse 2.4G2 FcγII/III (2.5 μg/ml) for 10 min and stained for 15 min with FITC-conjugated anti-mouse 7/4 (10 μg/ml; AbD Serotec) and PE-conjugated anti-mouse Ly6G (4 μg; BD Biosciences). Gates were constructed around two populations: the neutrophils (7/4^{high}, Ly6G^{high}) and inflammatory monocytes (7/4^{high}, Ly6G^{low}).

Statistics

Values for all measurements are expressed as mean ± SEM. The Student *t* test, one-way ANOVA with the Dunnett post hoc test, and two-way ANOVA with the Bonferroni post hoc test were performed to determine the levels of significance between groups using GraphPad Prism 5.0 software (GraphPad, San Diego, CA).

Results

C15 promotes phagocytosis of zymosan and OpZ in vitro

To determine the effect of C15 and control agents on MΦ phagocytosis of zymosan, MΦs were pretreated with 0.1 pM–1

nM C15 (AGEDPHGYFLPGQFA), C15-S (GLFHDQAGPPA-GYEF; scrambled C15 peptide), or chemerin for 45 min and challenged with zymosan-FITC over a 5–60-min time course. C15 elicited a dose-dependent increase in zymosan phagocytosis that was optimal at a dose of 10 pM (360% increase) at the 15-min time point (Fig. 1*A*, 1*C*, Supplemental Fig. 1*A*). Zymosan particles were readily phagocytosed by MΦs without opsonization; however, particles are unlikely to exist for extended periods in vivo without becoming opsonized. Therefore, we tested the effect of C15 on phagocytosis of OpZ. C15 induced a dose- and time-dependent increase in OpZ phagocytosis that was optimal with 10 pM C15 at the 15-min time point (230% increase; Fig. 1*B*, 1*D*).

Maximal phagocytosis occurred in vehicle-treated MΦs at 45-min postzymosan or OpZ challenge, whereas C15 (10 pM)-pretreated MΦs reached the saturation point at 15 min (Fig. 1*C*, 1*D*). At the 45- and 60-min time points, when vehicle- and C15-treated MΦ phagocytosis had reached a plateau, a 45% and 34% increase in zymosan and OpZ phagocytosis with C15 was noted (Fig. 1*C*, 1*D*). Thus, picomolar concentrations of C15 peptide enhanced the rate of MΦ zymosan uptake and increased overall MΦ phagocytic capacity for zymosan. The parent molecule, chemerin, and the control peptide, C15-S, had no effect on zymosan or OpZ phagocytosis by MΦs (Fig. 1*A*, 1*B*).

C15 promotes zymosan phagocytosis in a nonphlogistic manner

Phagocytosis of zymosan is a widely used model of microbial recognition by the innate immune system that typically results in MΦ activation and the secretion of proinflammatory cytokines (5, 26, 27). Given the prophagocytic effect of C15 on zymosan clearance, we determined whether C15 induces corresponding increases in inflammatory cytokine release in association with its effects on zymosan phagocytosis. In contrast, we found that C15-treated MΦs, which have phagocytosed up to 360% more zymosan, released reduced levels of proinflammatory cytokines and chemokines, including TNFα (53% decrease), IL-6 (48% decrease), IL-12 p40 (47% decrease), and JE (64% decrease), 15 h postphagocytosis (Fig. 1*E*). These data demonstrate that low picomolar doses of C15 peptide enhance zymosan phagocytosis in a nonphlogistic manner. To our knowledge, C15 peptide is the first mediator shown to induce phagocytosis of an inflammatory stimulus in a nonphlogistic manner. This may halt inflammation by removing the inciting stimulus and preventing the release of further proinflammatory mediators by MΦs.

C15 promotes nonphlogistic MΦ ingestion of apoptotic cells in vitro

MΦ phagocytosis of apoptotic cells is the classic example of phagocytic clearance without the provocation of an inflammatory response and is an important determinant of the resolution of inflammation (7, 9, 28). To probe the effect of chemerin-derived peptides on apoptotic cell phagocytosis in vitro, MΦs were pretreated with C15 (0.01–10 pM) for 45 min and then exposed to CFSE-labeled apoptotic Jurkat cells for 1 h. C15 enhanced MΦ phagocytosis of apoptotic cells with an optimal dose of 1 pM;

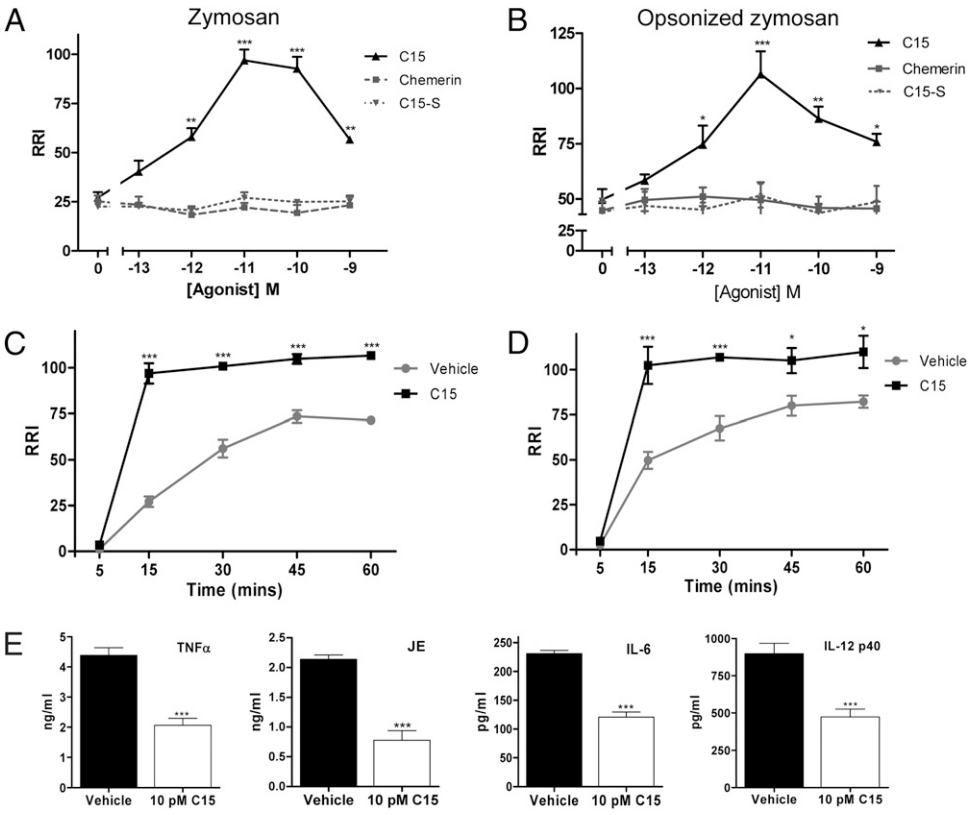

FIGURE 1. C15 promotes nonphlogistic phagocytosis of zymosan and OpZ in vitro. MΦs were pretreated with C15, C15-S, chemerin (0.1 pM–1 nM), or vehicle for 45 min, followed by a 15-min challenge with zymosan-FITC (*A*) or OpZ-FITC (*B*). MΦs were pretreated with C15 (10 pM) or vehicle for 45 min, followed by challenge with zymosan-FITC (*C*) or OpZ-FITC (*D*) for 5, 15, 30, 45, or 60 min. Noningested phagocytic targets were removed by thorough washing, and quantification of phagocytosed zymosan was carried out by FACS analysis. RRI = percentage of zymosan-FITC$^+$ MΦs × GeoMFI normalized to vehicle-treated samples; see *Materials and Methods* for a detailed description of the RRI. *E*, Effect of C15 on inflammatory cytokine production. MΦ supernatants were collected 15 h after ingestion of zymosan-FITC. TNF-α, JE, and IL-6 and -12 p40 levels were determined in cell supernatants using multiplex bead assays. Graphs show mean values ± SEM from four to eight independent experiments. $*p < 0.05$; $**p < 0.01$; $***p < 0.001$, relative to vehicle-treated samples. *A* and *B*, One-way ANOVA with the Dunnett post hoc test. *C* and *D*, Two-way ANOVA with Bonferroni post hoc test. *E*, Student *t* test.

a 247% increase in phagocytosis was observed (Fig. 2*A*, Supplemental Fig. 1*B*). However, similar prophagocytic effects were still seen with 0.1 pM C15: doses that are 10× and 100× lower than that required for optimal enhancement of zymosan and OpZ phagocytosis (Fig. 1*A*, 1*B*). We postulate that reduced C15 concentrations are required for optimal enhancement of apoptotic cell phagocytosis because C15 may act in concert with prophagocytic mediators that are known to be released by apoptotic cells, including nucleotides and Annexin A1 (29–31). Intriguingly, the parent protein chemerin, which failed to enhance zymosan ingestion (Fig. 1*A*), promoted phagocytosis of apoptotic cells with an optimal dose of 0.1 pM (Fig. 2*B*). These prophagocytic effects were abolished when chemerin was administered in the presence of the serine and cysteine protease inhibitor (leupeptin), demonstrating that chemerin promotes phagocytosis in a proteolysis-dependent manner (Fig. 2*B*). These data mirror our previous observations that chemerin suppresses MΦ activation in a proteolysis-dependent manner (25), suggesting that classically activated MΦs and apoptotic cells are capable of releasing proteases that cleave chemerin to generate anti-inflammatory and prophagocytic peptides. We postulate that chemerin is cleaved during this assay by apoptotic cell-derived proteases, because chemerin did not exert any prophagocytic effects on zymosan and OpZ phagocytosis (Fig. 1*A*, 1*B*). In addition, C15-treated MΦs, which had ingested up to 2.5-fold more apoptotic cells, released reduced levels of proinflammatory cytokines TNF-α (63%; Fig. 2*C*) and JE (54%; Fig. 2*D*) and exhibited increased TGF-β expression (108%; Fig. 2*E*) with an optimal dose of 1 pM C15.

ChemR23$^{-/-}$ MΦs exhibit impaired phagocytosis in response to C15

To assess the involvement of the G-protein coupled receptor ChemR23 in mediating C15 enhancement of zymosan and OpZ phagocytosis, we compared the effect of C15 on phagocytosis of these targets by wild-type and ChemR23$^{-/-}$ MΦs at the 15-min time point. The prophagocytic effects of C15 on zymosan phagocytosis were completely abolished in ChemR23$^{-/-}$ MΦs, indicating that C15-enhanced clearance of zymosan requires the involvement of ChemR23 (Fig. 3*A*). In contrast, ChemR23$^{-/-}$ MΦs displayed a 71% reduction in C15 enhancement of OpZ phagocytosis at the optimal 10-pM dose (Fig. 3*B*). These data suggest the existence of an additional C15R that may be required for optimal enhancement of OpZ clearance in vitro (Fig. 3*B*). Furthermore, the level of zymosan ($^{+/+}$, 22 RRI; $^{-/-}$, 20 RRI; Fig. 3*A*) and OpZ ($^{+/+}$, 49 RRI; $^{-/-}$, 51 RRI; Fig. 3*B*) phagocytosis in untreated wild-type and ChemR23$^{-/-}$ MΦs was of equivalent magnitude.

We next assessed the involvement of ChemR23 in mediating C15 enhancement of apoptotic cell clearance, finding that the prophagocytic effects of C15 on apoptotic cell phagocytosis were completely abolished in ChemR23$^{-/-}$ MΦs, indicating that C15-enhanced clearance of this phagocytic target also requires the involvement of ChemR23 (Fig. 3*C*). In addition, the basal level of apoptotic cell ingestion in ChemR23$^{-/-}$ MΦs (14.5 RRI) was significantly lower than that of wild-type MΦs (22.7 RRI), providing the first indication of a phenotype for ChemR23$^{-/-}$ MΦs in the absence of an inflammatory stimulus (25).

C15 enhances MΦ zymosan phagocytosis during peritonitis

We previously showed that C15 ameliorates zymosan-induced peritonitis, reducing leukocyte recruitment by up to 65%, with a concomitant suppression of inflammatory mediator expression (25). Having demonstrated that C15 is capable of enhancing zymosan phagocytosis in vitro, we next assessed the effect of C15 (8 pg/mouse; 0.32 ng/kg) on MΦ zymosan phagocytosis in vivo in the zymosan peritonitis model. PECs were analyzed for uptake of zymosan-FITC and expression of the MΦ marker F4/80 (32). The maximum level of MΦs engaged in the clearance of zymosan occurred in control animals 1 h postzymosan challenge, where 23% of total cells were zymosan^{+}F4/80^{+} (Fig. 4*A*, Supplemental Fig. 1*C*). A single 8-pg dose of C15 enhanced MΦ zymosan clearance by 38%, increasing the percentage of zymosan^{+}F4/80^{+} PECs to 34% (Fig. 4*A*). C15 also enhanced MΦ zymosan

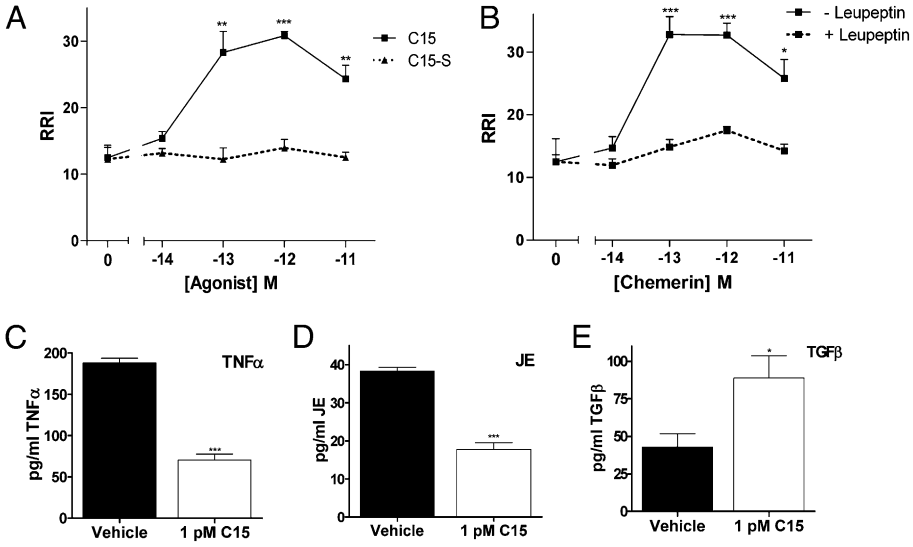

FIGURE 2. C15 and chemerin promote nonphlogistic phagocytosis of apoptotic cells in vitro. MΦs were pretreated with vehicle, C15, or C15-S (0.01–10 pM) (*A*) or chemerin (0.01–10 pM) ± leupeptin (10 μM) (*B*) for 45 min and then exposed to CFSE-labeled apoptotic Jurkat cells for 1 h. *C–E*, Effect of C15 on MΦ cytokine production following ingestion of apoptotic cells. TNF-α (*C*), JE (*D*), TGF-β (*E*), IL-6, and IL-12 p40 levels were determined in cell supernatants 15 or 24 h (TGF-β) following phagocytosis of apoptotic cells using multiplex bead assays and ELISA. IL-6 and -12 p40 levels were below the limit of detection for this assay (5 pg/ml). Noningested CFSE-labeled apoptotic cells and cell debris were removed by thorough washing, and quantification of ingested CFSE-labeled apoptotic cells was carried out by FACS analysis. Bar graphs show mean values ± SEM from four independent experiments. $*p < 0.05$; $**p < 0.01$; $***p < 0.001$; relative to vehicle-treated (*A*, *C–E*) or leupeptin-treated (*B*) samples. *A*, One-way ANOVA with the Dunnett post hoc test. *B*, Two-way ANOVA with Bonferroni post hoc test. *C–E*, Student *t* test.

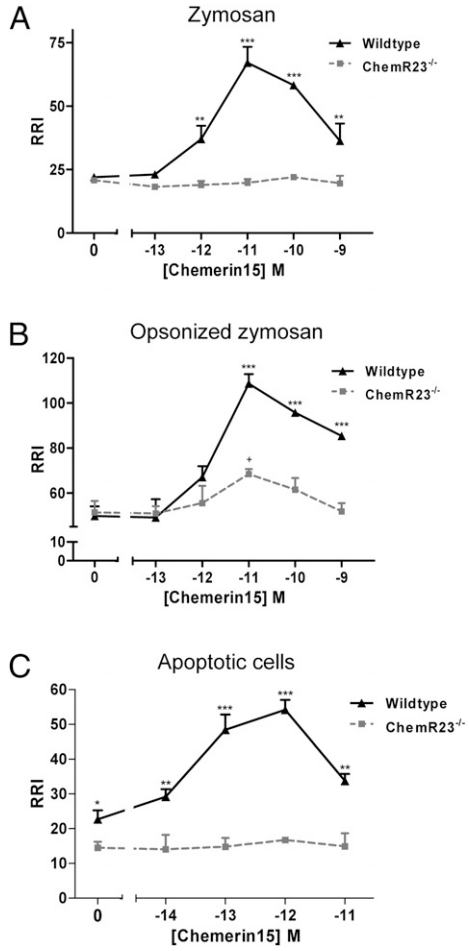

FIGURE 3. ChemR23$^{-/-}$ MΦs exhibit impaired phagocytosis in response to C15. Wild-type and ChemR23$^{-/-}$ MΦs on an Sv129 genetic background were pretreated with C15 (0.01 pM–1 nM) or vehicle for 45 min, followed by a 15-min challenge with zymosan-FITC (*A*) or OpZ-FITC (*B*) or a 1-h exposure to CFSE-labeled apoptotic cells (*C*). Non-ingested phagocytic targets were removed by thorough washing, and quantification of ingested zymosan, OpZ, and apoptotic cells was carried out by FACS analysis. Graphs show mean values ± SEM from four or five independent experiments. $*p < 0.05$; $**p < 0.01$; $***p < 0.001$, comparing wild-type MΦ C15 responses with ChemR23$^{-/-}$ MΦ C15 responses; two-way ANOVA with the Bonferroni post hoc test. $^{+}p < 0.05$, comparing ChemR23$^{-/-}$ MΦs treated with 10^{-11} M C15 with vehicle-treated ChemR23$^{-/-}$ MΦs; one-way ANOVA with the Dunnett post hoc test.

ingestion at 2 and 4 h postzymosan administration (Fig. 4*A*, 4*B*); this effect was not seen with the control peptide C15-S (Supplemental Fig. 2*A*).

C15 enhances phagocytosis of apoptotic neutrophils during inflammation

Constitutive apoptosis of neutrophils at inflammatory sites and their subsequent clearance by MΦs is a well-documented phenomenon and a critical determinant of inflammatory resolution. Failure to efficiently clear apoptotic cells can exacerbate inflammation because these cells will ultimately undergo secondary necrosis and lyse to release their histotoxic, proinflammatory, and immunogenic material (12, 23, 33, 34). Therefore, we assessed the effect of C15 on the clearance of apoptotic neutrophils in vivo during zymosan-induced peritoneal inflammation by analyzing PECs for the expression of the neutrophil marker Ly6G (35) and the MΦ marker F4/80 (32). We found that a single 8 pg/mouse dose of C15 enhanced Ly6G^{+} cell phagocytosis at the 8-h time point by 88% (Fig. 4*C*, Supplemental Fig. 1*D*). C15 also increased apoptotic neutrophil clearance at 2, 4, and 16 h (Fig. 4*C*, 4*D*), whereas the control peptide C15-S was unable to promote Ly6G^{+} cell phagocytosis (Supplemental Fig. 2*B*).

C15 enhances MΦ phagocytosis during peritonitis through ChemR23

We used ChemR23$^{-/-}$ mice to determine the ChemR23 dependency of C15's in vivo prophagocytic effects. C15 was unable to enhance MΦ phagocytosis of apoptotic neutrophils or zymosan in the absence of ChemR23, indicating that C15-enhanced clearance of apoptotic neutrophils and zymosan requires the involvement of ChemR23 (Fig. 4*E*, 4*F*). The basal level of MΦ zymosan engulfment in ChemR23$^{-/-}$ mice (4.8% cells zymosan^{+} F4/80^{+}) was indistinguishable from that of wild-type animals (4.9% zymosan^{+}F4/80^{+}; Fig. 4*E*). In contrast, ChemR23$^{-/-}$ mice exhibited a 27% deficit in apoptotic cell clearance compared with their wild-type counterparts when measured as the percentage of total cells. However, this effect is not seen when data are represented as the percentage of F4/80^{+} cells, indicating that the observed effect could be an artifact caused by differences in the numbers of F4/80^{+} cells in the peritoneal cavities of wild-type and ChemR23$^{-/-}$ cells, rather than a direct effect of ChemR23 ablation on phagocytosis (Fig. 4*F*). Taken together, our data support the conclusion that the chemerin peptide C15 is a potent stimulator of MΦ-mediated zymosan and apoptotic neutrophil phagocytosis in vivo through ChemR23.

C15 reduces levels of apoptotic and necrotic cells at the inflammatory site

We have clearly demonstrated the ability of C15 to potently enhance the clearance of apoptotic neutrophils in vivo; therefore, we next analyzed the effect of C15 on the level of apoptotic and necrotic cells at the inflammatory site during peritonitis. We used the standard approach of PI and Annexin V staining to quantitate apoptotic and necrotic cells in the peritoneal cavity. In control animals 4 h postzymosan challenge, apoptotic cells represented 18% of total PECs, whereas necrotic cells accounted for 4%. When mice were pretreated with a single 8-pg dose of C15, the percentage of apoptotic cells decreased by 31%, to 12% of total PECs (Fig. 5*A*, Supplemental Fig. 1), whereas the necrotic cell population was reduced by 53% to only 1.9% of total PECs (Fig. 5*B*, Supplemental Fig. 1*E*). These data indicate that the prophagocytic effects of C15 on apoptotic cell clearance result in a quantifiable reduction in the level of apoptotic cells present at the inflammatory site. This may then lead to the observed reduction in necrotic cells because fewer apoptotic cells escape phagocytic clearance and undergo secondary necrosis.

Our data show for the first time that the chemerin peptide C15 can promote inflammatory resolution through its ability to potently enhance apoptotic neutrophil phagocytosis during peritoneal inflammation in a ChemR23-dependent manner.

Blockade of endogenous chemerin species results in impaired phagocytosis in vivo

We assessed the role of endogenous chemerin peptides in phagocytosis and leukocyte recruitment during peritoneal inflammation using ChAb. We completed a zymosan-induced peritonitis time-course in which animals received pretreatment with control IgG or ChAb (100 ng/mouse) prior to a 0–48-h zymosan challenge. Neutralization of endogenous chemerin species resulted in elevated neutrophil and monocyte recruitment at all time points, except for the earliest (2 h), with a maximum increase of 170% (Fig. 6*A*, 6*B*). These data strongly support the existence of

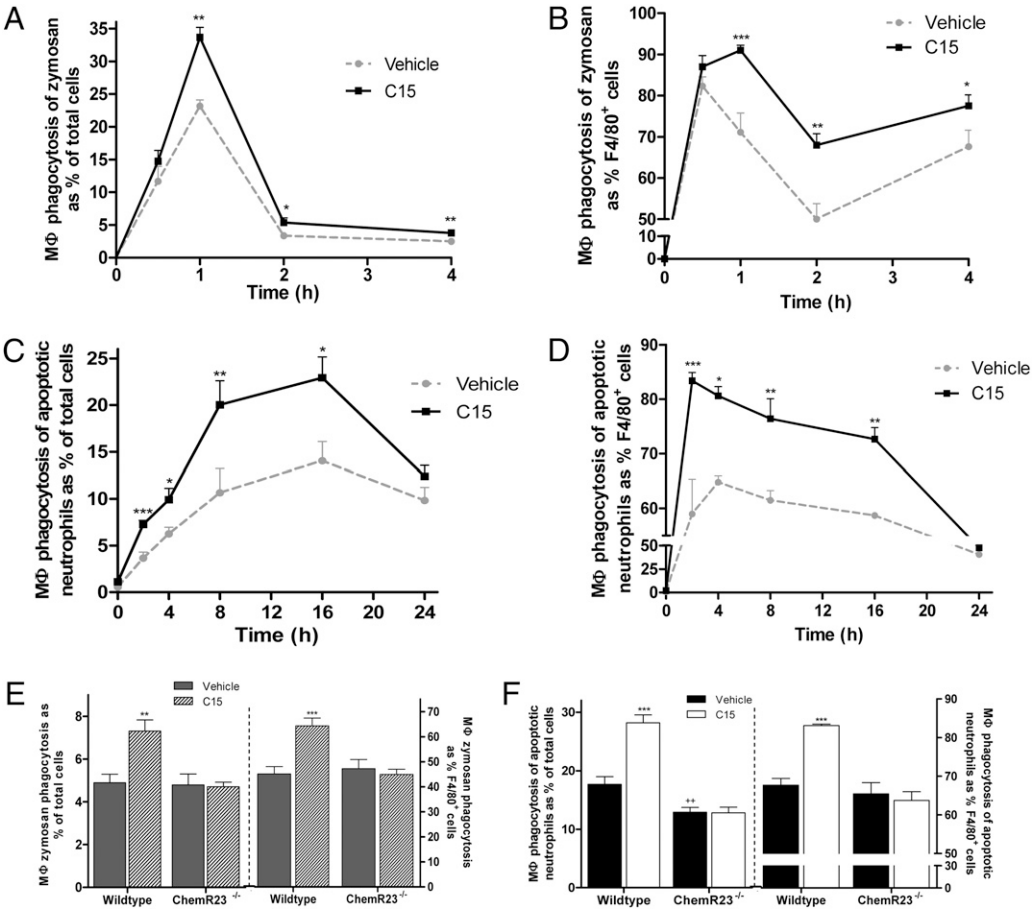

FIGURE 4. C15 enhances MΦ phagocytosis of zymosan and apoptotic neutrophils during peritonitis through ChemR23. *A* and *B*, C57BL/6 mice were dosed i.p with vehicle or C15 (0.32 ng/kg), followed by injection with zymosan-FITC 1 h later. PECs were harvested by peritoneal lavage at multiple time points postzymosan-FITC injection, permeabilized, and stained with anti-F4/80-Alexa Fluor 647. Zymosan$^+$F4/80$^+$ cells are expressed as the percentage of total cells (*A*) and as percentage of MΦs (F4/80$^+$ cells) (*B*), as determined by FACS analysis. *C* and *D*, C57BL/6 mice were dosed i.p with vehicle or C15 (0.32 ng/kg), followed by injection with zymosan 1 h later. PECs were harvested by peritoneal lavage at multiple time points postzymosan injection, permeabilized, and stained with anti–Ly6G-PE and anti–F4/80-Alexa Fluor 647. Ly6G$^+$F4/80$^+$ cells are expressed as the percentage of total cells (*C*) and as the percentage of MΦs (F4/80$^+$ cells) (*D*), as determined by FACS analysis. Graphs in *A–D* show mean values ± SEM, with 5–10 mice per treatment group (vehicle or C15) used at each time point. $*p < 0.05$; $**p < 0.01$; $***p < 0.001$, relative to vehicle-treated mice; two-way ANOVA with Bonferroni post hoc test. Sv129 and ChemR23$^{-/-}$ (Sv129) mice were dosed i.p with vehicle or C15 (0.32 ng/kg), followed by injection with zymosan-FITC (*E*) or zymosan (*F*) 1 h later. PECs were harvested by peritoneal lavage 4 h postzymosan-FITC administration to quantify zymosan$^+$F4/80$^+$ populations and 8 h post-zymosan administration to evaluate Ly6G$^+$F4/80$^+$ cell populations. PECs were permeabilized, stained, and analyzed as described in *A–D*. Graphs show mean values ± SEM for 6–12 mice per group. $**p < 0.01$; $***p < 0.001$; $^{++}p < 0.01$, relative to vehicle-treated wild-type mice.

anti-inflammatory chemerin-derived peptides in vivo that are involved in modulating leukocyte recruitment during peritoneal inflammation. In light of the potent prophagocytic effects of the chemerin peptide C15 on zymosan and apoptotic cell phagocytosis, we postulated that endogenous chemerin peptides may modulate the inflammatory response by promoting clearance of these phagocytic targets, in addition to suppressing leukocyte recruitment. Neutralization of endogenous chemerin species resulted in a reduction of up to 46% in zymosan phagocytosis (Fig. 6*C*, 6*D*) and Ly6G$^+$ cell (neutrophil) phagocytosis (Fig. 6*E*, 6*F*). These data provide evidence that endogenous chemerin species are an important component of the endogenous resolution system, involved in mediating the clearance of microbial particles and apoptotic cells in vivo.

C15 enhances phagocytosis and phagocytic cup formation through Syk-dependent changes in F-actin polymerization

Because C15 enhances the phagocytosis of multiple phagocytic targets, which are cargo for a variety of MΦ receptors, including dectin-1 for zymosan ingestion (36) and CD36 for apoptotic cell engulfment (37), it is likely that C15 enhances a common pathway of phagocytosis rather than having an effect on specific phagocytic receptor expression. This is particularly likely because FACS analysis showed no significant C15-elicited changes in dectin-1 expression during the course of the zymosan phagocytosis assay (data not shown), and C15 exerted no effect on MΦ binding of zymosan, as gauged by phagocytosis assays performed at 4°C (Supplemental Fig. 3).

Remodeling of the actin cytoskeleton is a prerequisite for phagocytosis, enabling the formation of phagocytic cups and, subsequently, the phagosome to internalize the phagocytic target (38–41). Therefore, we evaluated the effect of C15 on phagocytic cup formation and F-actin polymerization and localization. In addition, we further probed the mechanism by which C15 promotes phagocytosis using the Syk inhibitor PIC. Syk is a tyrosine kinase required for lysosome–phagosome fusion in unopsonized yeast phagocytosis (42), but it is not required for yeast or apoptotic cell internalization (43–45). In agreement with these observations, Syk inhibition had no effect on basal MΦ zymosan or apoptotic cell phagocytosis (Fig. 7*A*, 7*B*). However, pretreatment

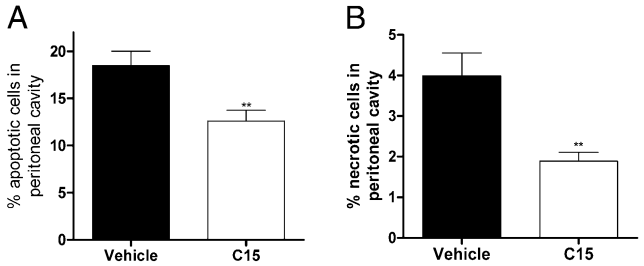

FIGURE 5. C15 reduces levels of apoptotic and necrotic cells at the inflammatory site. *A* and *B*, C57BL/6 mice were dosed i.p with vehicle or C15 (0.32 ng/kg), followed by injection with 10 μg zymosan 1 h later. PECs were harvested by peritoneal lavage 4 h postzymosan challenge, and the percentages of live, apoptotic (*A*) and necrotic (*B*) cells were determined by staining with annexin V-FITC and propidium iodide. Live cells were Annexin V^-PI^-, apoptotic cells were Annexin$^+PI^-$, and necrotic cells were Annexin V^+PI^+. Graphs show mean values ± SEM for five to seven mice per treatment group. $^{**}p < 0.01$, relative to vehicle-treated mice; Student *t* test.

of MΦs with PIC prior to C15 treatment resulted in complete abrogation of C15-induced enhancement of zymosan (Fig. 7*A*) and apoptotic cell phagocytosis (Fig. 7*B*). Therefore, these data demonstrate that C15 enhances zymosan and apoptotic cell phagocytosis in a Syk-dependent manner.

Subsequently, we probed the effect of C15 on phagocytic cup formation, finding that C15 treatment elicited a significant increase in the percentage of cells with phagocytic cups, from 25% of cells with vehicle treatment up to 40% of cells following treatment with 10 pM C15. This increase in phagocytic cup formation was completely abrogated by treatment with the Syk inhibitor PIC (Fig. 7*C*). Importantly, vehicle-treated and C15 + PIC-treated MΦs predominantly possessed early phagocytic cups, whereas higher levels of early phagosomes and late phagocytic cups were observed following C15 treatment (Supplemental Fig. 4). These data suggest that C15 may increase the kinetics of phagosome formation in a Syk-dependent manner. C15 also enhanced F-actin polymerization at the early phagocytic cup (Fig. 7*D*), the late phagocytic cup (Fig. 7*E*), and the early phagosome (Fig. 7*F*). C15-mediated alterations in local F-actin polymerization were inhibited by PIC, indicating an essential role for Syk in this process (Fig. 7*D–F*). In light of these observations, we assessed the effect of C15 on Syk activation, finding that C15 (10 pM) triggered phosphorylation of Syk (Tyr352) in a time-dependent manner (Supplemental Fig. 5). Since phagocytosis, phagocytic cup formation, and F-actin polymerization at the phagocytic cups and early phagosomes were enhanced by C15, and C15-mediated effects were abrogated by the Syk inhibitor PIC, we suggest that C15 enhances phagocytosis through Syk-mediated alterations in F-actin polymerization, which likely aid phagocytic cup formation and, thus, enhances MΦ phagocytosis.

Discussion

In this study, we identify the chemerin peptide C15 as a new mediator capable of promoting inflammatory resolution following microbial challenge by stimulating MΦ clearance of the inciting stimulus and apoptotic neutrophils in a nonphlogistic manner. Efficient clearance of invading microorganisms at sites of inflammation is an indispensible role of MΦs. The ability of C15 to potently enhance this process, in vitro and in vivo, further highlights the dynamic nature of the MΦ and its capacity for phagocytosis while providing novel insights into the regulation of innate immune responses by endogenous anti-inflammatory pathways.

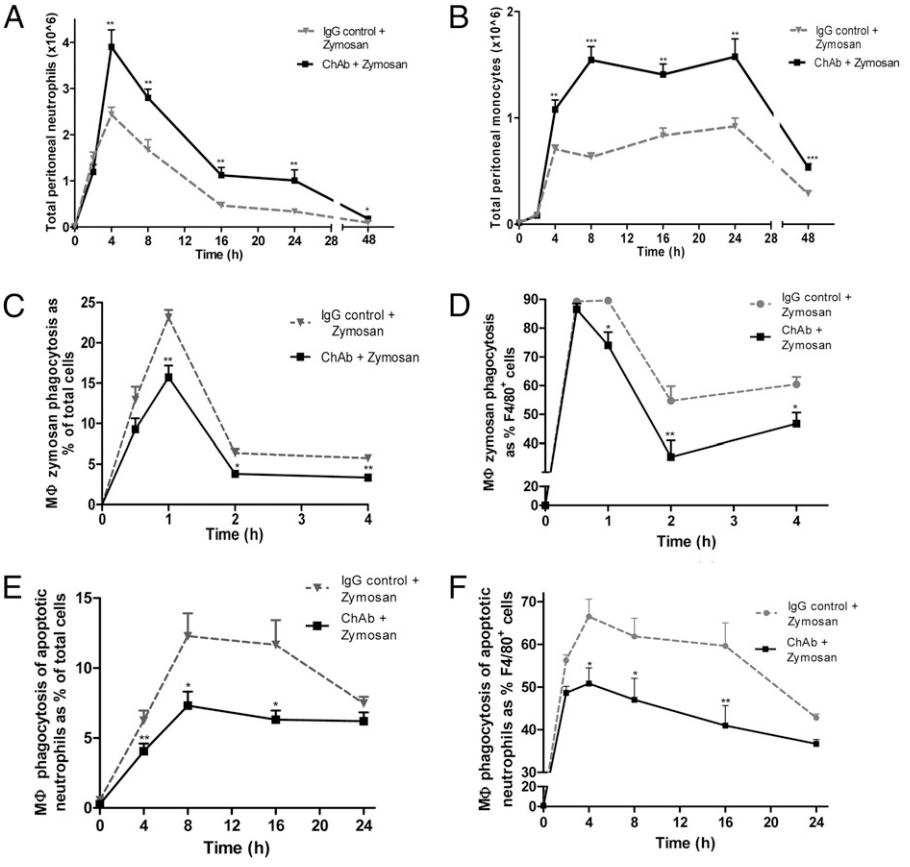

FIGURE 6. Neutralization of endogenous chemerin species results in elevated leukocyte recruitment and impaired phagocytosis in vivo. C57BL/6J mice were dosed i.p with ChAb (100 ng/mouse) or control IgG (100 ng/mouse), followed by injection with zymosan (10 μg/cavity) 1 h later. PECs were harvested at multiple time points postzymosan injection (*A*, *B*, *E*, *F*) or postzymosan-FITC injection (*C*, *D*). *A* and *B*, Total PECs were quantified, and cellular composition (neutrophils versus monocytes) was determined by FACS analysis. Cells were stained with Ly6G-PE and 7/4-FITC, and gates were constructed around two populations: neutrophils (*A*; $7/4^{high}$ $Ly6G^{high}$) and monocytes (*B*; $7/4^{high}Ly6G^{low}$). *C* and *D*, PECs were permeabilized and stained with anti–F4/80-Alexa Fluor 647, and the percentage of zymosan$^+$F4/80$^+$ cells was determined by FACS analysis. *E* and *F*, PECs were permeabilized and stained with anti–Ly6G-PE and anti–F4/80-Alexa Fluor 647, and the percentage of $Ly6G^+$, $F4/80^+$ cells was determined by FACS analysis. Graphs show mean values ± SEM for 5–10 mice per treatment group (IgG control or ChAb) per time point. $^*p < 0.05$; $^{**}p < 0.01$; $^{***}p < 0.001$, relative to control IgG-treated mice. Two-way ANOVA with Bonferroni post hoc test.

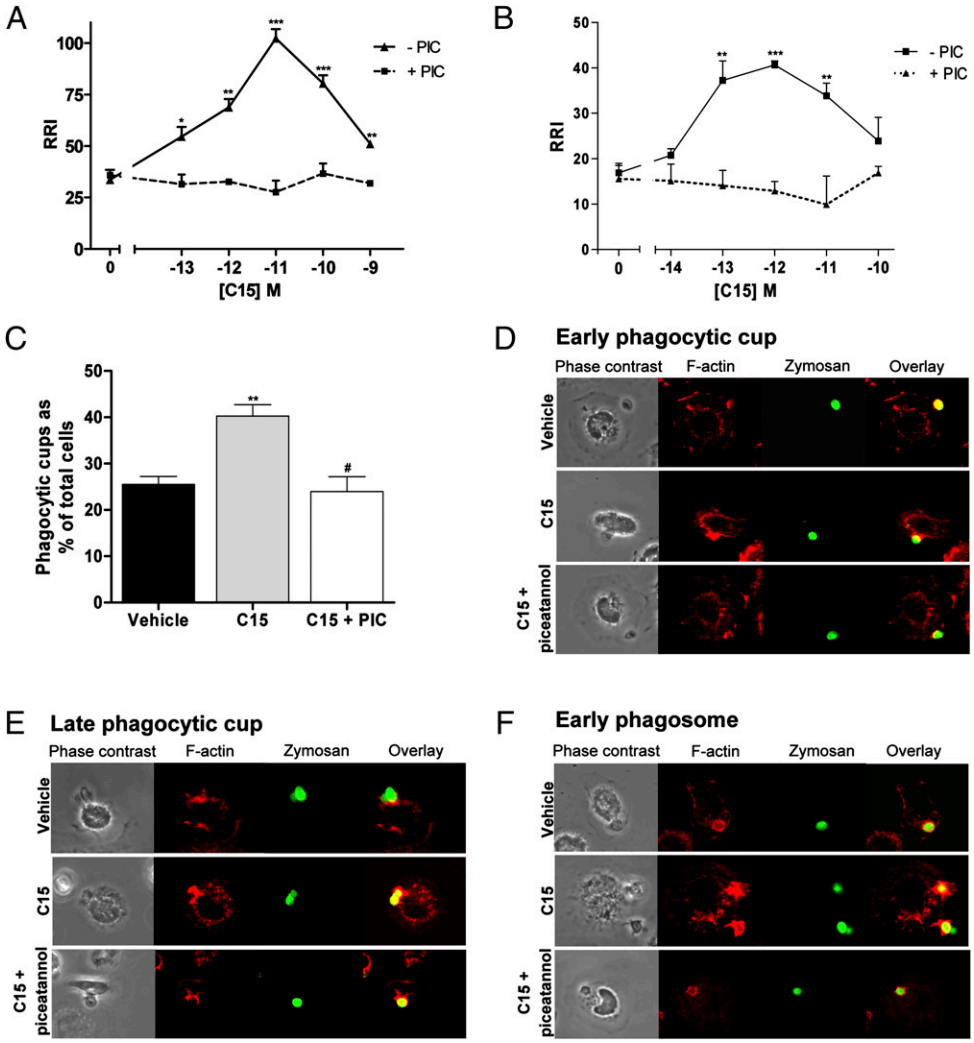

FIGURE 7. C15 enhances phagocytosis and phagocytic cup formation through Syk-dependent changes in F-actin polymerization. *A* and *B*, MΦs were pretreated with vehicle or PIC (10 μM) for 30 min followed by treatment with C15 (10^{-14}–10^{-9} M) or vehicle for 45 min. MΦs were subsequently challenged with zymosan-FITC for 15 min (*A*) or CFSE-labeled apoptotic Jurkat cells for 1 h (*B*). Samples were processed as in Fig. 1. *C–F*, MΦs were pretreated with vehicle or PIC for 30 min, followed by treatment with C15 (10 pM) or vehicle for 45 min and subsequent challenge with zymosan-FITC for 15 min (*C*) or 5 min (*D–F*). Cells were fixed and stained with Alexa Fluor 546-phalloidin to visualize polymerized actin, phagocytic cups, and phagosomes and viewed using a ×60 magnification. *C*, Early and late phagocytic cups were quantified and expressed as the percentage of total cells. Representative images of early phagocytic cups (*D*), late phagocytic cups (*E*), and early phagosomes (*F*) are shown. Figures show mean values ± SEM from three independent experiments. *A* and *B*, $^{**}p < 0.01$; $^{***}p < 0.001$, relative to PIC-treated samples; two-way ANOVA with the Bonferroni post hoc test. *C*, $^{**}p < 0.01$, relative to vehicle-treated samples; $^{\#}p < 0.05$, relative to C15-treated samples. One-way ANOVA with the Bonferroni posttest. Results were confirmed with a second Syk inhibitor BAY 61-3606 (data not shown).

Furthermore, this study indicates that manipulation of the chemerin peptide/ChemR23 axis may be an attractive avenue for therapeutic intervention in inflammation.

Perhaps the most striking characteristic of C15 is the dose at which it exerts its effects. C15 suppresses leukocyte recruitment by up to 65% (25) and enhances phagocytosis in vivo by up to 100% when administered in low picogram quantities. The lipid-resolution mediators resolvin E1, protectin D1, and lipoxin A_4 exert less dramatic effects at much higher doses (27). Although these mediators enhance zymosan phagocytosis (27), it is unknown whether this occurs in a nonphlogistic manner, whereas the prototypical anti-inflammatory drug dexamethasone inhibits MΦ zymosan phagocytosis (46). To our knowledge, C15 peptide is the first mediator shown to induce MΦ phagocytosis of an inflammatory stimulus in a nonphlogistic manner. This may halt inflammation by removing the inciting stimulus and preventing the release of further proinflammatory mediators by MΦs.

Interestingly, the dose required for optimal enhancement of apoptotic cell phagocytosis in vitro by C15 was 10-fold lower than that required for other phagocytic targets. This observation may reflect differences in the nature of these assays; phagocytosis of zymosan can be viewed as a proinflammatory event because MΦ activation and the release of proinflammatory mediators ensues, whereas apoptotic cell engulfment is a nonphlogistic process. Alternatively, apoptotic cells were shown to release prophagocytic signals, including Annexin A1 and Annexin-derived peptides (30), which could act in concert with the C15 peptide administered in this assay to promote MΦ clearance of apoptotic cells.

We have described for the first time a mechanism through which C15 enhances MΦ phagocytosis, which involves Syk-dependent changes in phagocytic cup formation and F-actin localization. $Syk^{-/-}$ MΦs, along with $DAP12^{-/-}$ MΦs, have been shown to display a phenotype characterized by elevated proinflammatory cytokine production in comparison with their wild-type counterparts

(47). It is plausible that C15 and endogenous chemerin species may harness this endogenous DAP12/Syk signaling pathway to elicit their anti-inflammatory and prophagocytic effects. If this is the case, 0Syk-deficient mice could be rendered unresponsive to C15 treatment.

We have demonstrated that the anti-inflammatory and prophagocytic effects of C15 are absent in ChemR23$^{-/-}$ MΦs and ChemR23$^{-/-}$ mice, but we were unable to detect a significant difference between zymosan-elicited neutrophil and monocyte recruitment in wild-type and ChemR23$^{-/-}$ at the 4-h time point (25). Therefore, it is intriguing that ChemR23 ablation also has no discernable effect on phagocytosis in vitro or in vivo, when we have clearly demonstrated that neutralization of endogenous chemerin species results in deficits in zymosan and apoptotic neutrophil phagocytosis. Our previous studies demonstrated that the full-length protein chemerin is cleaved into anti-inflammatory peptides that act on ChemR23, in addition to other unidentified receptor(s) (25). Thus, the absence of impaired phagocytosis in ChemR23$^{-/-}$ mice may be due to redundancy in the receptors for chemerin peptides in the anti-inflammatory/proresolution system. Additional receptors for chemerin, and potentially the chemerin peptides, are GPR1 and CCRL2 (48, 49). Therefore, ablation of the chemerin gene (RARRES-2) may result in mice with a more overt phenotype than the ChemR23$^{-/-}$ mice through the removal of chemerin-derived ligands for ChemR23 and other potential receptors.

Taken together, our novel data suggest that C15's potent anti-inflammatory effects in vivo are a result of a combination of direct suppression of MΦ activation (25) and enhancement of MΦ phagocytosis of the inciting stimulus and apoptotic neutrophils. We provide compelling evidence for the role of chemerin peptides and ChemR23 in MΦ phagocytosis and the resolution of inflammation. Therefore, manipulation of the chemerin peptide/ChemR23 axis may represent a novel therapeutic approach for the treatment of inflammatory pathologies, such as atherosclerosis and SLE, in which failure to efficiently clear apoptotic cell debris has been implicated in their pathogenesis (50).

Acknowledgments

We thank E. McNeil, P. Taylor, and G. White for advice.

Disclosures

The authors have no financial conflicts of interest.

References

1. Metchnikoff, E. 1887. Ueber den Kampf der Zellen gegen Erysipelkokken, ein Beitrag zur Phagocytenlehre. *Arch. Pathol. Anat.* [Virchow's Archiv.] 107: 209–249.
2. Gordon, S. 2007. The macrophage: past, present and future. *Eur. J. Immunol.* 37 (Suppl. 1): S9–S17.
3. Mosser, D. M., and J. P. Edwards. 2008. Exploring the full spectrum of macrophage activation. *Natl. Rev. Immunol.* 8: 958–969.
4. Rossi, A. G., D. A. Sawatzky, A. Walker, C. Ward, T. A. Sheldrake, N. A. Riley, A. Caldicott, M. Martinez-Losa, T. R. Walker, R. Duffin, et al. 2006. Cyclin-dependent kinase inhibitors enhance the resolution of inflammation by promoting inflammatory cell apoptosis. *Nat. Med.* 12: 1056–1064.
5. Taylor, P. R., S. V. Tsoni, J. A. Willment, K. M. Dennehy, M. Rosas, H. Findon, K. Haynes, C. Steele, M. Botto, S. Gordon, and G. D. Brown. 2007. Dectin-1 is required for beta-glucan recognition and control of fungal infection. *Nat. Immunol.* 8: 31–38.
6. Fadok, V. A., P. P. McDonald, D. L. Bratton, and P. M. Henson. 1998. Regulation of macrophage cytokine production by phagocytosis of apoptotic and post-apoptotic cells. *Biochem. Soc. Trans.* 26: 653–656.
7. Fadok, V. A., D. L. Bratton, A. Konowal, P. W. Freed, J. Y. Westcott, and P. M. Henson. 1998. Macrophages that have ingested apoptotic cells in vitro inhibit proinflammatory cytokine production through autocrine/paracrine mechanisms involving TGF-beta, PGE2, and PAF. *J. Clin. Invest.* 101: 890–898.
8. Fadok, V. A., D. L. Bratton, and P. M. Henson. 2001. Phagocyte receptors for apoptotic cells: recognition, uptake, and consequences. *J. Clin. Invest.* 108: 957–962.
9. Huynh, M. L., V. A. Fadok, and P. M. Henson. 2002. Phosphatidylserine-dependent ingestion of apoptotic cells promotes TGF-beta1 secretion and the resolution of inflammation. *J. Clin. Invest.* 109: 41–50.
10. Neumann, J., S. Sauerzweig, R. Rönicke, F. Gunzer, K. Dinkel, O. Ullrich, M. Gunzer, and K. G. Reymann. 2008. Microglia cells protect neurons by direct engulfment of invading neutrophil granulocytes: a new mechanism of CNS immune privilege. *J. Neurosci.* 28: 5965–5975.
11. Silva, M. T., A. do Vale, and N. M. dos Santos. 2008. Secondary necrosis in multicellular animals: an outcome of apoptosis with pathogenic implications. *Apoptosis* 13: 463–482.
12. Savill, J., I. Dransfield, C. Gregory, and C. Haslett. 2002. A blast from the past: clearance of apoptotic cells regulates immune responses. *Natl. Rev. Immunol.* 2: 965–975.
13. Vandivier, R. W., P. M. Henson, and I. S. Douglas. 2006. Burying the dead: the impact of failed apoptotic cell removal (efferocytosis) on chronic inflammatory lung disease. *Chest* 129: 1673–1682.
14. Serhan, C. N., and J. Savill. 2005. Resolution of inflammation: the beginning programs the end. *Nat. Immunol.* 6: 1191–1197.
15. Haslett, C. 1992. Resolution of acute inflammation and the role of apoptosis in the tissue fate of granulocytes. *Clin. Sci. (Lond.)* 83: 639–648.
16. Zhang, Z., G. Cherryholmes, and J. E. Shively. 2008. Neutrophil secondary necrosis is induced by LL-37 derived from cathelicidin. *J. Leukoc. Biol.* 84: 780–788.
17. Rock, K. L., and H. Kono. 2008. The inflammatory response to cell death. *Annu. Rev. Pathol.* 3: 99–126.
18. O'Brien, B. A., W. E. Fieldus, C. J. Field, and D. T. Finegood. 2002. Clearance of apoptotic beta-cells is reduced in neonatal autoimmune diabetes-prone rats. *Cell Death Differ.* 9: 457–464.
19. Cohen, P. L., R. Caricchio, V. Abraham, T. D. Camenisch, J. C. Jennette, R. A. Roubey, H. S. Earp, G. Matsushima, and E. A. Reap. 2002. Delayed apoptotic cell clearance and lupus-like autoimmunity in mice lacking the c-mer membrane tyrosine kinase. *J. Exp. Med.* 196: 135–140.
20. Munoz, L. E., U. S. Gaipl, S. Franz, A. Sheriff, R. E. Voll, J. R. Kalden, and M. Herrmann. 2005. SLE—a disease of clearance deficiency? *Rheumatology (Oxford)* 44: 1101–1107.
21. Gaipl, U. S., R. E. Voll, A. Sheriff, S. Franz, J. R. Kalden, and M. Herrmann. 2005. Impaired clearance of dying cells in systemic lupus erythematosus. *Autoimmun. Rev.* 4: 189–194.
22. Gaipl, U. S., L. E. Munoz, G. Grossmayer, K. Lauber, S. Franz, K. Sarter, R. E. Voll, T. Winkler, A. Kuhn, J. Kalden, et al. 2007. Clearance deficiency and systemic lupus erythematosus (SLE). *J. Autoimmun.* 28: 114–121.
23. Schrijvers, D. M., G. R. De Meyer, M. M. Kockx, A. G. Herman, and W. Martinet. 2005. Phagocytosis of apoptotic cells by macrophages is impaired in atherosclerosis. *Arterioscler. Thromb. Vasc. Biol.* 25: 1256–1261.
24. Ait-Oufella, H., V. Pouresmail, T. Simon, O. Blanc-Brude, K. Kinugawa, R. Merval, G. Offenstadt, G. Lesèche, P. L. Cohen, A. Tedgui, and Z. Mallat. 2008. Defective mer receptor tyrosine kinase signaling in bone marrow cells promotes apoptotic cell accumulation and accelerates atherosclerosis. *Arterioscler. Thromb. Vasc. Biol.* 28: 1429–1431.
25. Cash, J. L., R. Hart, A. Russ, J. P. Dixon, W. H. Colledge, J. Doran, A. G. Hendrick, M. B. Carlton, and D. R. Greaves. 2008. Synthetic chemerin-derived peptides suppress inflammation through ChemR23. *J. Exp. Med.* 205: 767–775.
26. Damazo, A. S., S. Yona, R. J. Flower, M. Perretti, and S. M. Oliani. 2006. Spatial and temporal profiles for anti-inflammatory gene expression in leukocytes during a resolving model of peritonitis. *J. Immunol.* 176: 4410–4418.
27. Schwab, J. M., N. Chiang, M. Arita, and C. N. Serhan. 2007. Resolvin E1 and protectin D1 activate inflammation-resolution programmes. *Nature* 447: 869–874.
28. Ren, Y., and J. Savill. 1998. Apoptosis: the importance of being eaten. *Cell Death Differ.* 5: 563–568.
29. Maderna, P., S. Yona, M. Perretti, and C. Godson. 2005. Modulation of phagocytosis of apoptotic neutrophils by supernatant from dexamethasone-treated macrophages and annexin-derived peptide Ac(2-26). *J. Immunol.* 174: 3727–3733.
30. Scannell, M., M. B. Flanagan, A. deStefani, K. J. Wynne, G. Cagney, C. Godson, and P. Maderna. 2007. Annexin-1 and peptide derivatives are released by apoptotic cells and stimulate phagocytosis of apoptotic neutrophils by macrophages. *J. Immunol.* 178: 4595–4605.
31. Elliott, M. R., F. B. Chekeni, P. C. Trampont, E. R. Lazarowski, A. Kadl, S. F. Walk, D. Park, R. I. Woodson, M. Ostankovich, P. Sharma, et al. 2009. Nucleotides released by apoptotic cells act as a find-me signal to promote phagocytic clearance. *Nature* 461: 282–286.
32. McKnight, A. J., A. J. Macfarlane, P. Dri, L. Turley, A. C. Willis, and S. Gordon. 1996. Molecular cloning of F4/80, a murine macrophage-restricted cell surface glycoprotein with homology to the G-protein-linked transmembrane 7 hormone receptor family. *J. Biol. Chem.* 271: 486–489.
33. Baumann, I., W. Kolowos, R. E. Voll, B. Manger, U. Gaipl, W. L. Neuhuber, T. Kirchner, J. R. Kalden, and M. Herrmann. 2002. Impaired uptake of apoptotic cells into tingible body macrophages in germinal centers of patients with systemic lupus erythematosus. *Arthritis Rheum.* 46: 191–201.
34. Ren, Y., J. Tang, M. Y. Mok, A. W. Chan, A. Wu, and C. S. Lau. 2003. Increased apoptotic neutrophils and macrophages and impaired macrophage phagocytic clearance of apoptotic neutrophils in systemic lupus erythematosus. *Arthritis Rheum.* 48: 2888–2897.
35. Daley, J. M., A. A. Thomay, M. D. Connolly, J. S. Reichner, and J. E. Albina. 2008. Use of Ly6G-specific monoclonal antibody to deplete neutrophils in mice. *J. Leukoc. Biol.* 83: 64–70.

36. Brown, G. D., and S. Gordon. 2001. Immune recognition. A new receptor for beta-glucans. *Nature* 413: 36–37.
37. Fadok, V. A., M. L. Warner, D. L. Bratton, and P. M. Henson. 1998. CD36 is required for phagocytosis of apoptotic cells by human macrophages that use either a phosphatidylserine receptor or the vitronectin receptor (alpha v beta 3). *J. Immunol.* 161: 6250–6257.
38. Sheterline, P., J. E. Rickard, and R. C. Richards. 1984. Fc receptor-directed phagocytic stimuli induce transient actin assembly at an early stage of phagocytosis in neutrophil leukocytes. *Eur. J. Cell Biol.* 34: 80–87.
39. Greenberg, S., J. el Khoury, F. di Virgilio, E. M. Kaplan, and S. C. Silverstein. 1991. Ca(2+)-independent F-actin assembly and disassembly during Fc receptor-mediated phagocytosis in mouse macrophages. *J. Cell Biol.* 113: 757–767.
40. Greenberg, S. 1999. Modular components of phagocytosis. *J. Leukoc. Biol.* 66: 712–717.
41. May, R. C., and L. M. Machesky. 2001. Phagocytosis and the actin cytoskeleton. *J. Cell Sci.* 114: 1061–1077.
42. Majeed, M., E. Caveggion, C. A. Lowell, and G. Berton. 2001. Role of Src kinases and Syk in Fcgamma receptor-mediated phagocytosis and phagosome-lysosome fusion. *J. Leukoc. Biol.* 70: 801–811.
43. Canetti, C., B. Hu, J. L. Curtis, and M. Peters-Golden. 2003. Syk activation is a leukotriene B4-regulated event involved in macrophage phagocytosis of IgG-coated targets but not apoptotic cells. *Blood* 102: 1877–1883.
44. Herre, J., A. S. Marshall, E. Caron, A. D. Edwards, D. L. Williams, E. Schweighoffer, V. Tybulewicz, C. Reis e Sousa, S. Gordon, and G. D. Brown. 2004. Dectin-1 uses novel mechanisms for yeast phagocytosis in macrophages. *Blood* 104: 4038–4045.
45. Underhill, D. M., E. Rossnagle, C. A. Lowell, and R. M. Simmons. 2005. Dectin-1 activates Syk tyrosine kinase in a dynamic subset of macrophages for reactive oxygen production. *Blood* 106: 2543–2550.
46. Mlambo, G., and L. B. Sigola. 2003. Rifampicin and dexamethasone have similar effects on macrophage phagocytosis of zymosan, but differ in their effects on nitrite and TNF-alpha production. *Int. Immunopharmacol.* 3: 513–522.
47. Hamerman, J. A., N. K. Tchao, C. A. Lowell, and L. L. Lanier. 2005. Enhanced toll-like receptor responses in the absence of signaling adaptor DAP12. *Nat. Immunol.* 6: 579–586.
48. Zabel, B. A., S. Nakae, L. Zúñiga, J.-Y. Kim, T. Ohyama, C. Alt, J. Pan, H. Suto, D. Soler, S. J. Allen, et al. 2008. Mast cell-expressed orphan receptor CCRL2 binds chemerin and is required for optimal induction of IgE-mediated passive cutaneous anaphylaxis. *J. Exp. Med.* 205: 2207–2220.
49. Barnea, G., W. Strapps, G. Herrada, Y. Berman, J. Ong, B. Kloss, R. Axel, and K. J. Lee. 2008. The genetic design of signaling cascades to record receptor activation. *Proc. Natl. Acad. Sci. USA* 105: 64–69.
50. Aprahamian, T., I. Rifkin, R. Bonegio, B. Hugel, J. M. Freyssinet, K. Sato, J. J. Castellot, Jr., and K. Walsh. 2004. Impaired clearance of apoptotic cells promotes synergy between atherogenesis and autoimmune disease. *J. Exp. Med.* 199: 1121–1131.